Optimizing the Latent Space of Generative Networks

Piotr Bojanowski [1] **Armand Joulin** [1] **David Lopez Paz** [1] **Arthur Szlam** [1]

Abstract

Generative Adversarial Networks (GANs) have achieved remarkable results in the task of generating realistic natural images. In most successful applications, GAN models share two common aspects: solving a challenging saddle point optimization problem, interpreted as an adversarial game between a generator and a discriminator functions; and parameterizing the generator and the discriminator as deep convolutional neural networks. The goal of this paper is to disentangle the contribution of these two factors to the success of GANs. In particular, we introduce *Generative Latent Optimization* (GLO), a framework to train deep convolutional generators using simple reconstruction losses. Throughout a variety of experiments, we show that GLO enjoys many of the desirable properties of GANs: synthesizing visually-appealing samples, interpolating meaningfully between samples, and performing linear arithmetic with noise vectors; all of this without the adversarial optimization scheme.

1. Introduction

Generative Adversarial Networks (GANs) (Goodfellow et al., 2014) are a powerful framework to learn models capable of generating natural images. GANs learn these generative models by setting up an adversarial game between two learning machines. On the one hand, a generator plays to transform noise vectors into fake samples, which resemble real samples drawn from a distribution of natural images. On the other hand, a discriminator plays to distinguish between real and fake samples. During training, the generator and the discriminator functions are optimized in turns. First, the discriminator learns to assign high scores to real samples, and low scores to fake samples. Then, the generator learns to increase the scores of fake samples, so as to "fool" the discriminator. After proper training, the generator is able to produce realistic natural images from noise vectors.

Recently, GANs have been used to produce high-quality images resembling handwritten digits, human faces, and house interiors (Radford et al., 2015). Furthermore, GANs exhibit three strong signs of generalization. First, the generator translates *linear interpolations in the noise space* into *semantic interpolations in the image space*. In other words, a linear interpolation in the noise space will generate a smooth interpolation of visually-appealing images. Second, the generator allows *linear arithmetic in the noise space*. Similarly to word embeddings (Mikolov et al., 2013), linear arithmetic indicates that the generator organizes the noise space to disentangle the nonlinear factors of variation of natural images into linear statistics. Third, the generator is able to to synthesize new images that resemble those of the data distribution. This allows for applications such as image in-painting (Iizuka et al., 2017) and super-resolution (Ledig et al., 2016).

Despite their success, training and evaluating GANs is notoriously difficult. The adversarial optimization problem implemented by GANs is sensitive to random initialization, architectural choices, and hyper-parameter settings. In many cases, a fair amount of human care is necessary to find the correct configuration to train a GAN in a particular dataset. It is common to observe generators with similar architectures and hyper-parameters to exhibit dramatically different behaviors. Even when properly trained, the resulting generator may synthesize samples that resemble only a few localized regions (or modes) of the data distribution (Goodfellow, 2017). While several advances have been made to stabilize the training of GANs (Salimans et al., 2016), this task remains more art than science.

The difficulty of training GANs is aggravated by the challenges in their evaluation: since evaluating the likelihood of a GAN with respect to the data is an intractable problem, the current gold standard to evaluate the quality of GANs is to eyeball the samples produced by the generator. This qualitative evaluation gives little insight on the coverage of the generator, making the mode dropping issue hard to measure. The evaluation of discriminators is also difficult, since their visual features do not always transfer well to

[1]Facebook AI Research. Correspondence to: Piotr Bojanowski <bojanowski@fb.com>.

Proceedings of the 35^{th} International Conference on Machine Learning, Stockholm, Sweden, PMLR 80, 2018.

supervised tasks (Donahue et al., 2016; Dumoulin et al., 2016). Finally, the application of GANs to non-image data has been relatively limited.

1.1. Research question

To model natural images with GANs, the generator and discriminator are commonly parametrized as deep Convolutional Networks (convnets) (LeCun et al., 1998). Therefore, it is reasonable to hypothesize that the reasons for the success of GANs in modeling natural images come from two complementary sources:

(A1) Leveraging the powerful inductive bias of deep convnets.

(A2) The adversarial training protocol.

This work attempts to disentangle the factors of success (A1) and (A2) in GAN models. Specifically, we propose and study one algorithm that relies on (A1) and avoids (A2), but still obtains competitive results when compared to a GAN.

Contributions. We investigate the importance of the inductive bias of convnets by removing the adversarial training protocol of GANs (Section 2). Our approach, called *Generative Latent Optimization* (GLO), maps one *learnable* noise vector to each of the images in our dataset by minimizing a simple reconstruction loss. Since we are predicting *images from learnable noise*, GLO borrows inspiration from recent methods to predict *learnable noise from images* (Bojanowski & Joulin, 2017). Alternatively, one can understand GLO as an auto-encoder where the latent representation is not produced by a parametric encoder, but learned freely in a non-parametric manner. In contrast to GANs, we track the correspondence between each learned noise vector and the image that it represents. Hence, the goal of GLO is to find a meaningful organization of the noise vectors, such that they can be mapped to their target images. To turn GLO into a generative model, we observe that it suffices to learn a simple probability distribution on the learned noise vectors.

We study the efficacy of GLO to compress and decompress a dataset of images, generate new samples, perform linear interpolations and extrapolations in the noise space, and perform linear arithmetic. Our experiments provide quantitative and qualitative comparisons to Principal Component Analysis (PCA), Variational Autoencoders (VAE) and GANs. Our results show that on many image datasets, in particular CelebA, MNIST and SVHN, the celebrated properties of GAN generations can be reproduced without the GAN training protocol. On the other hand, our qualitative results on the LSUN bedrooms are worse than the results of GANs; we hypothesize (and show evidence) that this is a capacity issue. It has been observed that GANs are prone to mode collapse, completely forgetting large parts of the training dataset. In the literature this is often described as a problem with the GAN training procedure. Our experiments suggest that this is more of a feature than a bug, as it allows relatively small models to generate realistic images by intelligently choosing which part of the data to ignore. We quantitatively measure the significance of this issue with a reconstruction criterion.

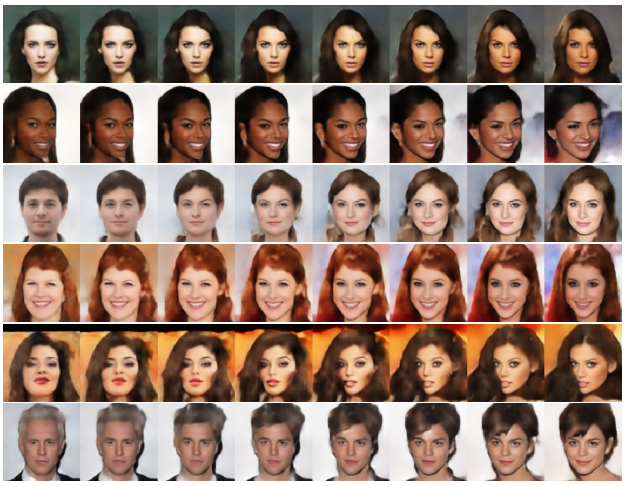

Figure 1. Illustration of interpolations obtained with our model on the CelebA dataset. Each row corresponds to an image pair, and the leftmost and rightmost images are actual images from the training set. Given two images i and j, we get interpolated latent vectors z between z_i and z_j and show the reconstruction $g(z)$.

2. The Generative Latent Optimization

First, we consider a large set of images $\{x_1, \dots, x_N\}$, where each image $x_i \in \mathcal{X}$ has dimensions $3 \times w \times h$. Second, we initialize a set of d-dimensional random vectors $\{z_1, \dots, z_N\}$, where $z_i \in \mathcal{Z} \subseteq \mathbb{R}^d$ for all $i = 1, \dots N$. Third, we pair the dataset of images with the random vectors, obtaining the dataset $\{(z_1, x_1), \dots, (z_N, x_N)\}$. Finally, we jointly learn the parameters θ in Θ of a generator $g_\theta : \mathcal{Z} \to \mathcal{X}$ and the optimal noise vector z_i for each image x_i, by solving:

$$\min_{\theta \in \Theta} \frac{1}{N} \sum_{i=1}^{N} \left[\min_{z_i \in \mathcal{Z}} \ell\left(g_\theta(z_i), x_i\right) \right], \qquad (1)$$

In the previous, $\ell : \mathcal{X} \times \mathcal{X}$ is a loss function measuring the reconstruction error from $g(z_i)$ to x_i. We call this model Generative Latent Optimization (GLO).

Learnable z_i. In contrast to autoencoders (Bourlard & Kamp, 1988), which assume a parametric model $f : \mathcal{X} \to \mathcal{Z}$, usually referred to as the *encoder*, to compute the vector z from samples x, and minimize the reconstruction

loss $\ell(g(f(x)), x)$, in GLO we jointly optimize the inputs $z_1, \ldots, z_N$ and the model parameter θ. Since the vector z is a free parameter, our model can recover all the solutions that could be found by an autoencoder, and reach some others. In a nutshell, GLO can be viewed as an "encoderless" autoencoder, or as a "discriminator-less" GAN.

Choice of $\mathcal{Z}$. A common choice of $\mathcal{Z}$ in the GAN literature is from a Normal distribution on $\mathbb{R}^d$. Since random vectors z drawn from the d-dimensional Normal distribution are very unlikely to land far outside the (surface of) the sphere $\mathcal{S}(\sqrt{d}, d, 2)$, and since projection onto the sphere is easy and numerically pleasant, after each z update in GLO training we project onto the sphere. For simplicity, instead of using the $\sqrt{d}$ sphere, we use the unit sphere.

Choice of loss function. On the one hand, the squared-loss function $\ell_2(x, x') = \|x - x'\|_2^2$ is a simple choice, but leads to blurry (average) reconstructions of natural images. On the other hand, GANs use a convnet (the discriminator) as loss function. Since the early layers of convnets focus on edges, the samples from a GAN are sharper. Therefore, our experiments provide quantitative and qualitative comparisons between the ℓ_2 loss and the Laplacian pyramid Lap_1 loss

$$\text{Lap}_1(x, x') = \sum_j 2^{2j} |L^j(x) - L^j(x')|_1,$$

where $L^j(x)$ is the j-th level of the Laplacian pyramid representation of x (Ling & Okada, 2006). Therefore, the Lap_1 loss weights the details at fine scales more heavily. In order to preserve low-frequency content such as color information, we will use a weighted combination of the Lap_1 and the ℓ_2 costs.

Optimization. For any choice of differentiable generator, the objective (1) is differentiable with respect to z, and θ. Therefore, we will learn z and θ by Stochastic Gradient Descent (SGD). The gradient of (1) with respect to z can be obtained by backpropagating the gradients through the generator function (Bora et al., 2017). We project each z back to the representation space $\mathcal{Z}$ after each update. To have noise vectors laying on the unit ℓ_2 sphere, we project z after each update by dividing its value by $\max(\|z\|_2, 1)$. We initialize z by sampling them from a Gaussian distribution.

Generator architecture. Among the multiple architectural variations explored in the literature, the most prominent is the Deep Convolutional Generative Adversarial Network (DCGAN) (Radford et al., 2015). Therefore, in this paper, to make the comparison with the GAN literature as straightforward as possible, we will use the generator function of DCGAN construct the generator of GLO across all of our experiments.

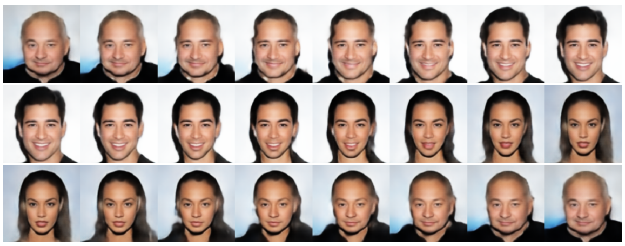

Figure 2. Illustration of interpolations obtained with our model on the CelebA dataset. We construct a path between 3 images to verify that paths do not collapse to an "average" representation in the middle of the interpolation.

3. Related work

Generative Adversarial Networks. GANs were introduced by Goodfellow et al. (2014), and refined in multiple recent works (Denton et al., 2015; Radford et al., 2015; Zhao et al., 2016; Salimans et al., 2016). As described in Section 1, GANs construct a generative model of a probability distribution P by setting up an adversarial game between a generator g and a discriminator d:

$$\min_G \max_D \mathbb{E}_{x\sim P} \log d(x) + \mathbb{E}_{z\sim Q} (1 - \log d(g(z))).$$

In practice, most of the applications of GANs concern modeling distributions of natural images. In these cases, both the generator g and the discriminator d are parametrized as deep convnets (LeCun et al., 1998).

Autoencoders. In their simplest form, an Auto-Encoder (AE) is a pair of neural networks, formed by an encoder $f : \mathcal{X} \to \mathcal{Z}$ and a decoder $g : \mathcal{Z} \to \mathcal{X}$. The role of an autoencoder is the compress the data $\{x_1, \ldots, x_N\}$ into the representation $\{z_1, \ldots, z_N\}$ using the encoder $f(x_i)$, and decompress it using the decoder $g(f(x_i))$. Therefore, autoencoders minimize $\mathbb{E}_{x\sim P} \ell(g(f(x)), x)$, where $\ell : \mathcal{X} \times \mathcal{X}$ is a simple loss function, such as the mean squared error. There is a vast literature on autoencoders, spanning three decades from their conception (Bourlard & Kamp, 1988; Baldi & Hornik, 1989), renaissance (Hinton & Salakhutdinov, 2006), and recent probabilistic extensions (Vincent et al., 2008; Kingma & Welling, 2013).

Several works have combined GANs with AEs. For instance, Zhao et al. (2016) replace the discriminator of a GAN by an AE, and Ulyanov et al. (2017) replace the decoder of an AE by a generator of a GAN. Similar to GLO, these works suggest that the combination of standard pipelines can lead to good generative models. In this work we attempt one step further, to explore if learning a generator alone is possible.

Inverting generators. Several works attempt at recovering the latent representation of an image with respect to a generator. In particular, Lipton & Tripathi (2017); Zhu et al. (2016) show that it is possible to recover z from a *generated*

Figure 3. Illustration of feature arithmetic on the CelebA dataset. We show that by taking the average hidden representation of the first row (man with sunglasses), substracting the one of the second row (men without sunglasses) and adding the one of the third row (women without sunglasses), we obtain a coherent image.

sample. Similarly, Creswell & Bharath (2016) show that it is possible to learn the inverse transformation of a generator. These works are similar to (Zeiler & Fergus, 2014), where the gradients of a particular feature of a convnet are backpropagated to the pixel space in order to visualize what that feature stands for. From a theoretical perspective, Bruna et al. (2013) explore the theoretical conditions for a network to be invertible. All of these inverting efforts are instances of the *pre-image problem*, (Kwok & Tsang, 2004).

Bora et al. (2017) have recently showed that it is possible to recover from a trained generator with compressed sensing. Similar to our work, they use a ℓ_2 loss and backpropagate the gradient to the low rank distribution. However, they do not train the generator simultaneously. Jointly learning the representation and training the generator allows us to extend their findings. Santurkar et al. (2017) also use generative models to compress images.

Several works have used an optimization of a latent representation for the express purpose of generating realistic images, e.g. (Portilla & Simoncelli, 2000; Nguyen et al., 2017). In these works, the total loss function optimized to generate is trained separately from the optimization of the latent representation (in the former, the loss is based on a complex wavelet transform, and in the latter, on separately trained autoencoders and classification convolutional networks). In this work we train the latent representations and the generator together from scratch; and show that at test time we may sample new z either using simple parametric distributions or interpolations in the latent space.

Learning representations. Arguably, the problem of learning representations from data in an unsupervised manner is one of the long-standing problems in machine learning (Bengio et al., 2013; LeCun et al., 2015). One of the earliest algorithms used to achieve is goal is Principal Component Analysis, or PCA (Pearson, 1901; Jolliffe, 1986). For instance, PCA has been used to learn low-dimensional representations of human faces (Turk & Pentland, 1991), or to produce a hierarchy of features (Chan et al., 2015). The nonlinear extension of PCA is an autoencoder (Baldi & Hornik, 1989), which is in turn one of the most extended algorithms to learn low-dimensional representations from data. Similar algorithms learn low-dimensional representations of data with certain structure. For instance, in sparse coding (Aharon et al., 2006; Mairal et al., 2008), the representation of one image is the linear combination of a very few elements from a dictionary of features. More recently, Zhang et al. (2016) realized the capability of deep neural networks to map large collections of images to noise vectors, and Bojanowski & Joulin (2017) exploited a similar procedure to learn visual features unsupervisedly. Similarly to us, Bojanowski & Joulin (2017) allow the noise vectors z to move in order to better learn the mapping from images to noise vectors. The proposed GLO is the analogous to these works, in the opposite direction: learn a map *from* noise vectors *to* images. Finally, the idea of mapping between images and noise to learn generative models is a well known technique (Chen & Gopinath, 2000; Laparra et al., 2011; Sohl-Dickstein et al., 2015; Bordes et al., 2017).

Nuisance Variables. One might consider the generator parameters the variables of interest, and Z to be "nuisance variables". There is a classical literature on dealing with nuisance parameters while estimating the parameters of interest, including optimization methods as we have used (Stuart & Ord, 2010). In this framing, it may be better to marginalize over the nuisance variables, but for the models and data we use this is intractable.

Speech and music generation. Optimizing a latent representation of a generative model has a long history in speech (Rabiner & Schafer, 2007), both for fitting single examples in the context of fitting a generative model, and in the context of speaker adaptation. In the context of music generation and harmonazation, the first model was introduced by Ebcioğlu (1988). Closer to our work, is the neural network-based model of Hild et al. (1992), which was later improved upon by Hadjeres & Pachet (2017).

4. Experiments

In this section, we compare GLO quantitatively and qualitatively against standard generative models on a variety of datasets. We consider several tasks to understand the strengths and weaknesses of each model: a qualitative analysis of the properties of the latent space typically observed with deep generative models and an image reconstruction problem to give some quantitative insights on the capability of GLO to cover a dataset. We selected datasets that are both small and large, uni-modal and multi-modal to stress the specificities of our models in different settings.

	MNIST		SVHN		CelebA				LSUN			
	32		32		64		128		64		128	
method	train	test	train	test	train	test	train	test	train	test	train	test
PCA	20.6	20.3	30.2	30.3	25.1	25.1	23.6	23.6	23.6	23.7	21.9	22.0
VAE	26.2	25.7	27.9	27.8	25.0	24.9	26.2	25.0	23.8	23.8	22.1	22.1
DCGAN	26.9	27.2	30.2	30.1	25.0	25.0	23.5	23.5	21.8	21.9	20.8	20.9
GLO	27.0	27.2	30.7	30.7	27.7	27.7	26.4	26.4	24.8	24.9	22.0	22.1
VAE	25.3	25.0	24.5	24.5	22.8	22.8	23.4	23.2	22.1	22.1	20.6	20.6
DCGAN	25.8	26.2	26.0	26.0	21.9	21.9	21.3	21.3	19.0	19.1	18.7	18.7
GLO	26.2	26.2	27.9	28.0	25.5	25.6	24.7	24.8	23.3	23.4	21.4	21.4

Table 1. pSNR of reconstruction for different models. Below the line, the codes were found using Lap_1 loss (although the test error is still measured in pSNR). Above the line, the codes were found using mean square error. Note that the generators of the VAE and GLO models were trained to reconstruct in Lap_1 loss. pSNR of GAN reconstruction of images generated by GAN (not real images) is greater than 50.

Implementation details The generator of a GLO follows the same architecture as the generator of DCGAN. We use Stochastic Gradient Descent (SGD) to optimize both θ and z, setting the learning rate for θ at 1 and the learning rate of z at 10. After each update, the noise vectors z are projected to the unit ℓ_2 Sphere. In the sequel, we initialize the random vectors of GLO using a Gaussian distribution (for the CelebA dataset) or the top d principal components (for the LSUN dataset). We use the $\ell_2 + \text{Lap}_1$ loss for all the experiments but MNIST where we use an MSE loss.

4.1. Baselines and datasets.

We consider three standard baselines: PCA, VAE, and GAN. PCA (Pearson, 1901) is equivalent to a linear autoencoder (Baldi & Hornik, 1989). We use for VAE and GAN the same generator architecture as for GLO, i.e., a DCGAN. We also set the number of principal components for PCA to be same as the dimensions of the latent spaces. We use 32 dimensions for MNIST, 64 dimensions for SVHN and 256 dimensions for CelebA and LSUN. We use the same $\ell_2 + \text{Lap}_1$ loss for VAE as for GLO for all the experiments but MNIST where we use an MSE loss. For the rest, we train VAE with the default hyper-parameters for 25 epochs. We train the GAN baseline with the default hyper-parameters and many seeds.

For our empirical evaluation, we consider four varied image datasets. We select both "unimodal" and "multimodal" datasets to probe the difficulty of models in each setting. We carry out our experiments on MNIST [1], SVHN[2] as well as more challenging datasets such as CelebA[3] and LSUN-bedroom[4]. On smaller datasets (MNIST and SVHN), we keep the images 32 pixels large. For CelebA and LSUN we resize the images to either 64 and 128 pixels large. For each dataset, we set aside evenly-spaced images corresponding to $\frac{1}{32}$ of the data, and consider these images as a test set. We train our models on the complement.

[1] http://yann.lecun.com/exdb/mnist/

[2] http://ufldl.stanford.edu/housenumbers/

[3] http://mmlab.ie.cuhk.edu.hk/projects/CelebA.html

[4] http://lsun.cs.princeton.edu/2017/

4.2. Properties of the latent space

The latent space of GANs seems to linearize the space of images. That is: interpolations between a pair of z vectors in the latent space map through the generator to a semantically meaningful, smooth nonlinear interpolation in image space. Figure 1 shows that the latent space of GLO seems to linearize the image space as well. For example, the model interpolates between examples that are geometrically quite different, reconstructing the rotation of the head from left to right, as well as interpolating between genders or different ages. It is important to note that these paths do not go through an "average" image of the dataset as the path interpolation between the 3 images of Figure 2 shows.

Linear arithmetic operations in the latent space of GANs can lead to meaningful image transformations. For example: (man with sunglasses - man + woman) produces an image of a woman with sunglasses. Figure 3 shows that the latent space of GLO shares the same property.

Finally, GLO models have the attractive property that the principal vectors corresponding to the largest principal values are meaningful in image space. As shown in Figure 6, they carry information like background color, the orientation of the head and gender. Interestingly, the gender information is represented by two principal vectors, one for the female and one for the male.

These results suggest that the desirable linearization properties of generators are probably due to the structure of the model (convnets) rather than the training procedure.

(a) MNIST (b) SVHN

(c) CelebA-64 (d) CelebA-128

(e) LSUN-64 (f) LSUN-128

Figure 4. Samples generated by VAE, DCGAN and GLO on the 4 datasets. For CelebA and LSUN, we consider images of size 64 and 128. On small datasets, the three models generate images of the comparable quality. On LSUN, images from VAE and GLO are nowhere close to those from DCGAN.

4.3. Generation

Another celebrated aspect of GANs is the high quality of the examples they generate. To sample from a GLO model, we fit a single full-covariance Gaussian to the Z found by the training procedure; and then pass samples from that Gaussian through the generator. Figure 4 shows a comparison between images generated by VAE, GAN and GLO models trained on different datasets, offering a few insights on the main difference between the methods: First, the images produced by VAE are often less sharp than GLO, in particular on large datasets like CelebA and LSUN bedroom. This observation suggests that the prior distribution on the latent space of a VAE may be too strong to fit many images, while vectors in the latent space of GLO move freely and use as much space as required to fit the images in the latent space. On the other hand, on these datasets, the trained Z from GLO are Gaussian enough to produce decent generations when fit with a single (full-covariance) Gaussian.

Second, it is interesting to notice that on the LSUN bedrooms, VAE and GLO are much worse than GAN. While they seem to capture the general shape of the bedrooms, they fail to produce the same level of detail as is observed in the samples generated by a GAN. One possibility is that in these settings, the "mode dropping" problem commonly discussed in the GAN literature (Goodfellow, 2017) is more a feature than a bug. Both VAE and GLO do not suffer from mode dropping by construction (since their loss forces them to reconstruct the whole dataset) and it is possible that as a result, they both generate poorly when the variability in the distribution increases relative to the model capacity. In other words, when confronted with more data variability than it can handle, a GAN can still be successful in generating (and well-organizing) a well-chosen subset of the data.

In the next section, we look at the reconstruction error of each method on the different datasets. This quantitative evaluation gives further insights on the differences between the approaches, and in particular, it gives evidence that GANs are not covering the training data.[5]

[5]Here "reduced" or "not covering" may be in the sense of missing some examples, for example dropping a cluster from a Gaussian mixture model, or more subtle retreats from the full data, for example projecting onto some complicated sub-manifold. We believe understanding precisely what reduction happens (if any) in

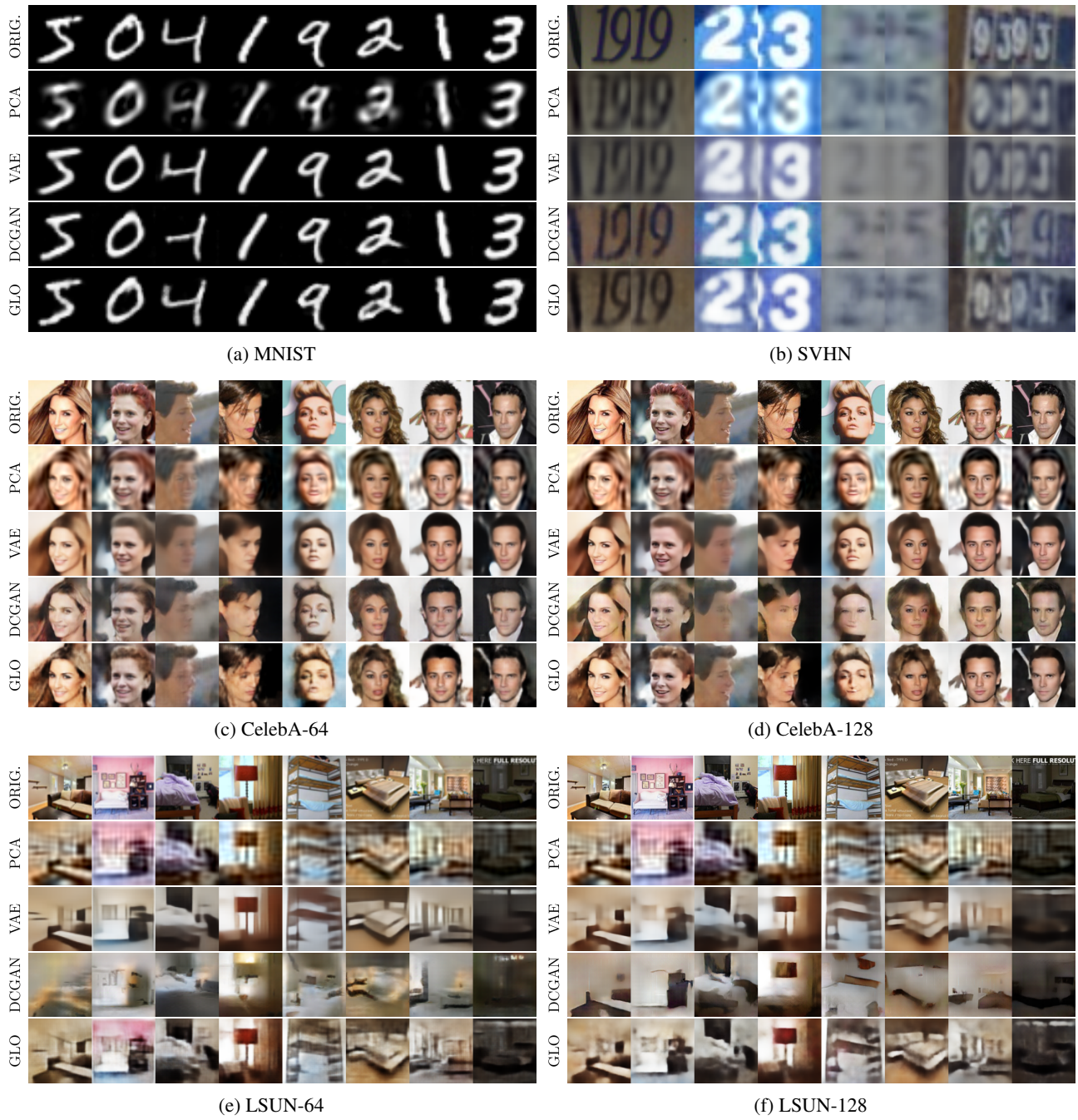

(a) MNIST (b) SVHN

(c) CelebA-64 (d) CelebA-128

(e) LSUN-64 (f) LSUN-128

Figure 5. Reconstruction results from PCA, VAE, DCGAN and GLO on the 4 datasets. The original images are on the top row. VAE reconstructions are blurrier than GLO . DCGAN fails to reconstruct images from large datasets.

4.4. Image reconstruction

In this set of experiments, we evaluate the quality of image reconstructions for each method. In Table 1 we report the reconstruction error in pSNR, which for a given image I and a reconstruction R, is defined as:

$$\text{pSNR}(I, R) = -20 \log_{10} \frac{\text{MAX}(I)}{\sqrt{\text{MSE}(I, R)}}, \qquad (2)$$

where MAX corresponds to the maximal value the image I can attain, and MSE is the Mean Squared Error.

To reconstruct an image from the test set, we need to find its latent representation. For the PCA and VAE baselines, this

the case of GANs trained with convnets on images is an exciting direction for future work.

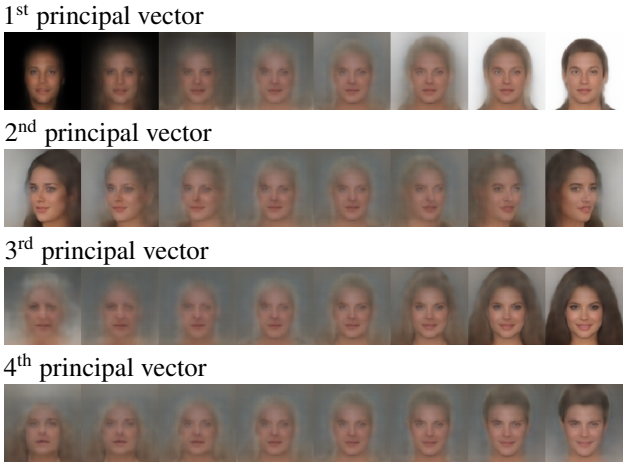

Figure 6. Interpolation from the average face along the principal vectors corresponding to the largest principal values. The principal vectors and values were computed on the (centered) Z vectors of the GLO model. The first vector seems to capture the brightness of the background, the second one the orientation of the face, while the third and forth capture the information about the gender. The average image is 4th from left.

is straightforward. The latent codes for DCGAN and GLO can be found by backpropagating the reconstruction error to the code through the generator. Note that the generating functions of *all* the GLO and VAE models in the table were trained with Lap_1 cost. This discrepancy in training loss favors PCA and if we find codes using MSE for GLO and DCGAN instead of Lap_1, the scores improve by $1-2$ points, even though we did not train GLO with an MSE.

Measuring a reconstruction error favors VAE and GLO over DCGAN as they are trained to minimize such an error metric. However, it is interesting to notice that on small datasets, there is no clear difference with DCGAN. The difference in performance between DCGAN and the other methods increases with the size of the dataset. This result already suggests that as the dataset grows, GANs are probably focusing on a subset of it, while, by objective, VAE and GLO are forced to reconstruct the full dataset. It is not clear though what is the nature of this "subset", as the distribution of the pSNR scores of a DCGAN is not significantly different from those of VAE or GLO as shown in the supplementary material. Finally, we remark although it is a-priori possible that the process of finding codes via backpropagation is not succeeding with the GAN generators, we find in practice that when we reconstruct an image *generated by the GAN*, the results are nearly perfect (pSNR > 50). This suggests that the difference in pSNR between the models is not due to poor optimization of the codes.

Figure 5 shows qualitative examples of reconstruction. As suggested by the quantitative results, the VAE reconstruction is much blurrier than GLO and the reconstruction quality of DCGAN quickly deteriorates with the size and variability of the dataset. More interestingly, on CelebA, we observe that, while DCGAN reconstructions of frontal faces look good, DCGAN struggles on side faces as well as rare examples, e.g., stylistic or blurry images. More important, they seem to be copy-pasting "faces" rather than reconstructing them. This effect is even more apparent on LSUN where it is almost impossible to find an entire well reconstructed image. However, even though the colors are off, the edges are sharp if they are reconstructed, suggesting that GANs are indeed focusing on some specificities of the image distribution.

5. Discussion

The experimental results presented in this work suggest that, when working with images, we can recover many of the properties of GANs using convnets trained with a simple reconstruction losses. While this does not invalidate the promise of GANs as generic models of uncertainty or as methods for building generative models, our results suggest that, in order to further test the adversarial construction, research needs to move beyond images modeled using convnets. On the other hand, practitioners who care only about generating images for a particular application, and find that the parameterized discriminator does improve their results, can incorporate reconstruction losses in their models, alleviating some of the instability of adversarial training.

While the visual quality of our results are promising, especially on the CelebA dataset, they are not yet to the level of the results obtained by GANs on the LSUN bedrooms. This suggests that being able to cover the entire dataset is too onerous of a task if all that is required is to generate a few nice samples. In that respect, we see that GANs have trouble reconstructing randomly chosen images at the same level of fidelity as their generations. At the same time, GANs can produce good images after a single pass through the data with SGD, suggesting that the so-called "mode dropping" can be seen as a feature. In future work we hope to better understand the tension between these two observations, and clarify the definition of this phenomenon.

There are many possibilities for improving the quality of GLO samples beyond understanding the effects of coverage. For example other loss functions (e.g. a VGG metric, as in (Nguyen et al., 2017)), model architectures, especially progressive generation (Karras et al., 2017), and more sophisticated sampling methods after training the model all may improve the visual quality GLO samples. Finally, because the methods keep track of the correspondence between samples and their representatives, we hope to be able to organize the Z in interesting ways as we train.

References

Aharon, M., Elad, M., and Bruckstein, A. rmk-svd: An algorithm for designing overcomplete dictionaries for sparse representation. *IEEE Transactions on signal processing*, 2006.

Baldi, P. and Hornik, K. Neural networks and principal component analysis: Learning from examples without local minima. *Neural networks*, 1989.

Bengio, Y., Courville, A., and Vincent, P. Representation learning: A review and new perspectives. *IEEE transactions on pattern analysis and machine intelligence*, 35(8): 1798–1828, 2013.

Bojanowski, P. and Joulin, A. Unsupervised Learning by Predicting Noise. In *ICML*, 2017.

Bora, A., Jalal, A., Price, E., and Dimakis, A. G. Compressed Sensing using Generative Models. *arXiv preprint arXiv:1703.03208*, 2017.

Bordes, F., Honari, S., and Vincent, P. Learning to Generate Samples from Noise through Infusion Training. *arXiv preprint arXiv:1703.06975*, 2017.

Bourlard, H. and Kamp, Y. Auto-association by multilayer perceptrons and singular value decomposition. *Biological cybernetics*, 1988.

Bruna, J., Szlam, A., and LeCun, Y. Signal recovery from pooling representations. *arXiv preprint arXiv:1311.4025*, 2013.

Chan, T.-H., Jia, K., Gao, S., Lu, J., Zeng, Z., and Ma, Y. PCANet: A Simple Deep Learning Baseline for Image Classification? *IEEE Transactions on Image Processing*, 2015.

Chen, S. S. and Gopinath, R. A. Gaussianization. In *NIPS*, 2000.

Creswell, A. and Bharath, A. A. Inverting The Generator Of A Generative Adversarial Network. *arXiv preprints arXiv:1611.05644*, 2016.

Denton, E. L., Chintala, S., Szlam, A., and Fergus, R. Deep generative image models using a laplacian pyramid of adversarial networks. In *NIPS*, 2015.

Donahue, J., Krähenbühl, P., and Darrell, T. Adversarial feature learning. *arXiv preprint arXiv:1605.09782*, 2016.

Dumoulin, V., Belghazi, I., Poole, B., Lamb, A., Arjovsky, M., Mastropietro, O., and Courville, A. Adversarially learned inference. *arXiv preprint arXiv:1606.00704*, 2016.

Ebcioğlu, K. An expert system for harmonizing four-part chorales. *Computer Music Journal*, 12(3):43–51, 1988.

Goodfellow, I. NIPS 2016 Tutorial: Generative Adversarial Networks. *arXiv preprint arXiv:1701.00160*, 2017.

Goodfellow, I., Pouget-Abadie, J., Mirza, M., Xu, B., Warde-Farley, D., Ozair, S., Courville, A., and Bengio, Y. Generative adversarial nets. In *NIPS*, 2014.

Hadjeres, G. and Pachet, F. Deepbach: a steerable model for bach chorales generation. *ICML*, 2017.

Hild, H., Feulner, J., and Menzel, W. Harmonet: A neural net for harmonizing chorales in the style of js bach. In *NIPS*, 1992.

Hinton, G. E. and Salakhutdinov, R. R. Reducing the dimensionality of data with neural networks. *Science*, 2006.

Iizuka, S., Simo-Serra, E., and Ishikawa, H. Globally and Locally Consistent Image Completion. *ACM Transactions on Graphics*, 36(4):107:1–107:14, 2017.

Jolliffe, I. T. *Principal component analysis and factor analysis*. Springer, 1986.

Karras, T., Aila, T., Laine, S., and Lehtinen, J. Progressive growing of gans for improved quality, stability, and variation. *arXiv preprint arXiv:1710.10196*, 2017.

Kingma, D. P. and Welling, M. Auto-encoding variational bayes. *arXiv preprint arXiv:1312.6114*, 2013.

Kwok, J.-Y. and Tsang, I.-H. The pre-image problem in kernel methods. *IEEE transactions on neural networks*, 2004.

Laparra, V., Camps-Valls, G., and Malo, J. Iterative gaussianization: from ica to random rotations. *IEEE transactions on neural networks*, 2011.

LeCun, Y., Bottou, L., Bengio, Y., and Haffner, P. Gradient-based learning applied to document recognition. *Proceedings of the IEEE*, 1998.

LeCun, Y., Bengio, Y., and Hinton, G. Deep learning. *Nature*, 2015.

Ledig, C., Theis, L., Huszár, F., Caballero, J., Cunningham, A., Acosta, A., Aitken, A., Tejani, A., Totz, J., Wang, Z., et al. Photo-realistic single image super-resolution using a generative adversarial network. *arXiv preprint arXiv:1609.04802*, 2016.

Ling, H. and Okada, K. Diffusion distance for histogram comparison. In *CVPR*, 2006.

Lipton, Z. C. and Tripathi, S. Precise Recovery of Latent Vectors from Generative Adversarial Networks. *arXiv preprints arXiv:1702.04782*, 2017.

Mairal, J., Elad, M., and Sapiro, G. Sparse representation for color image restoration. *IEEE Transactions on Image Processing*, 2008.

Mikolov, T., Chen, K., Corrado, G., and Dean, J. Efficient estimation of word representations in vector space. *arXiv preprint arXiv:1301.3781*, 2013.

Nguyen, A., Yosinski, J., Bengio, Y., Dosovitskiy, A., and Clune, J. Plug & play generative networks: Conditional iterative generation of images in latent space. In *CVPR*, 2017.

Pearson, K. On lines and planes of closest fit to systems of points in space. *The London, Edinburgh, and Dublin Philosophical Magazine and Journal of Science*, 1901.

Portilla, J. and Simoncelli, E. P. A parametric texture model based on joint statistics of complex wavelet coefficients. *International journal of computer vision*, 40(1):49–70, 2000.

Rabiner, L. R. and Schafer, R. W. Introduction to digital speech processing. *Foundations and Trends in Signal Processing*, 1(1/2):1–194, 2007.

Radford, A., Metz, L., and Chintala, S. Unsupervised Representation Learning with Deep Convolutional Generative Adversarial Networks. *arXiv preprint arXiv:1511.06434*, 2015.

Salimans, T., Goodfellow, I., Zaremba, W., Cheung, V., Radford, A., and Chen, X. Improved techniques for training gans. In *NIPS*, 2016.

Santurkar, S., Budden, D., and Shavit, N. Generative compression. *arXiv preprint arXiv:1703.01467*, 2017.

Sohl-Dickstein, J., Weiss, E. A., Maheswaranathan, N., and Ganguli, S. Deep unsupervised learning using nonequilibrium thermodynamics. *arXiv preprint arXiv:1503.03585*, 2015.

Stuart, A. and Ord, K. *Kendall's Advanced Theory of Statistics*. Wiley, 2010.

Turk, M. A. and Pentland, A. P. Face recognition using eigenfaces. In *CVPR*, 1991.

Ulyanov, D., Vedaldi, A., and Lempitsky, V. Adversarial Generator-Encoder Networks. *arXiv preprints arXiv:1704.02304*, 2017.

Vincent, P., Larochelle, H., Bengio, Y., and Manzagol, P.-A. Extracting and composing robust features with denoising autoencoders. In *ICML*, 2008.

Zeiler, M. D. and Fergus, R. Visualizing and understanding convolutional networks. In *ECCV*, 2014.

Zhang, C., Bengio, S., Hardt, M., Recht, B., and Vinyals, O. Understanding deep learning requires rethinking generalization. *arXiv preprint arXiv:1611.03530*, 2016.

Zhao, J., Mathieu, M., and LeCun, Y. Energy-based generative adversarial network. *arXiv preprint arXiv:1609.03126*, 2016.

Zhu, J.-Y., Krähenbühl, P., Shechtman, E., and Efros, A. A. Generative visual manipulation on the natural image manifold. In *ECCV*, 2016.